

# MODELING OF OFF-GAS AND PARTICLES FLOW UNDER ROOF OF A CLOSED SUBMERGED ARC FURNACE

M. Kadkhodabeigi<sup>1</sup>, B. Ravary<sup>1</sup> and D. O. Hjertenes<sup>2</sup>

<sup>1</sup> R&D department of Eramet Norway AS, 7037 Trondheim, Norway; Mehdi.kadkhodabeigi@erametgroup.com and Benjamin.ravary@erametgroup.com

<sup>2</sup> Eramet Norway Sauda AS, 4201 Sauda, Norway; Dag-ole.hjertenes@erametgroup.com

## ABSTRACT

*Eramet Norway operates closed submerged arc furnaces (SAFs) for production of ferroalloys such as Ferromanganese (FeMn) and Silicomanganese (SiMn). Smelting process generates large amount of high temperature process gasses in the SAF's bottom part. The gasses then move upwards through available void spaces between the charge particles in the furnace and, after taking part in different gas-solid reactions, reach the charge surface where they leave the furnace through off-gas ducts. Furnace off-gas is composed of different gas species and very fine particles of charge materials. The furnace off-gas is treated in off-gas system. Stability of the furnace operation is therefore depended on performance of the off-gas system. In order to improve efficiency of the furnace off-gas system, it is necessary to have a better understanding of the off-gas and particles flow in the system under different operational conditions. In the present work CFD model of an industrial size submerged arc furnace used for production of FeMn has been developed. The model simulates flow of off-gas and fine particles in the first part of the furnace off-gas system which starts from the charge surface (under the furnace roof) and ends up before the venturi gas scrubbers which are used for particles removal and off-gas cleaning. Results of simulation provide information about off-gas velocity, temperature and pressure together with particles distribution both under the furnace roof and in the off-gas channel. The model also determines areas of the system with high potential for particles accumulation and clogging. The results have been validated versus industrial measurements and observations such as off-gas pressure under the furnace roof, off-gas temperature in the off-gas channel and particles accumulation in the system.*

## 1 INTRODUCTION

Eramet Norway AS produces different grades of FeMn and SiMn in closed submerged arc furnaces. The closed submerged arc furnace has less power consumption (kwh/ton) and higher productivity compared to open furnace [1]. On the other hand, the requirements for ore used in closed furnace are more stringent [1]. Production of manganese alloys in the submerged arc furnaces results in generation of several byproducts such as slag, off-gas, sludge and diffuse emissions. Sustainable production of manganese alloys considering HSE (Health, Safety and Environment) has always been first priority in Eramet Norway. Therefore taking care of the above mentioned byproducts in a good way is always an important mission for us in Norway. Furnace off-gas handling system is an important part of a submerged arc furnace. The furnace off-gas systems in Eramet Norway are composed of different parts including off-gas uptakes on the furnace roof, dry zone, venturi scrubbers, filter and MRU (Mercury Recovery Unit). In fact the gas of the furnace operation, which is a mixture of different gas species such as CO, CO<sub>2</sub>, H<sub>2</sub>, N<sub>2</sub>, O<sub>2</sub> and fine particles of raw materials, is treated by the off-gas system. A schematic of the furnace off-gas system which is used in one of furnaces in Eramet Norway is shown in Figure 1. This figure shows position of the off-gas uptakes on the furnace roof, the first section of the furnace off-gas system (before the venturi system) and venturi gas scrubbers (in three stages). The furnace off-gas flows through this path towards MRU facility as the last part of the off-gas handling system.

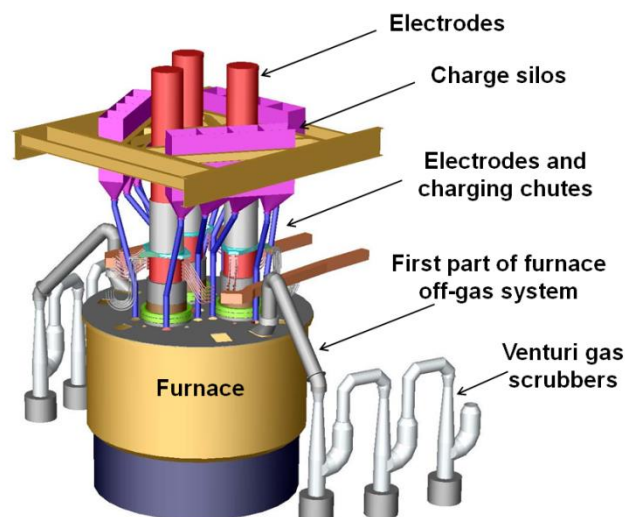


**Figure 1:** Schematic view of a submerged arc furnace and its off-gas handling system

Since occurrence of any problem in the off-gas system can lead to stoppage of the furnace operation, optimal operation of the off-gas system is vital for a stability of furnace operation. Therefore having a reliable and efficient off-gas system is very important from operational, environmental and economic points of view. In addition, dust from the furnace off-gas which is collected in the venturi scrubbers results in generation of a sludge which is deposited at a cost. Any modifications from the furnace roof design or operational procedures which reduce sludge quantity can have important extra economic benefits.

Regarding operation of the furnace off-gas systems there are several issues such as off-gas pressure control, particles removal in the gas scrubbers and accumulation of particles and tars both in the furnace freeboard (distance between charge surface and the roof) and in different zones of the off-gas handling system. Operational experiences prove that any changes in the raw materials and/or operational conditions of the furnace lead to a change in the properties of the furnace off-gas such as temperature, pressure, off-gas volume, concentration of tars and fine particles in the off-gas.

Control of the off-gas pressure in freeboard of the furnace is, for example, very important in closed submerged arc furnaces. The main reason is that existence of high pressure off-gas in the freeboard can lead to leakages of the off-gas from any small opening on the furnace roof. Since CO (g) is one of the main components in the off-gas, any leakage on the furnace roof can be dangerous. In our furnaces there are one or several sampling point in the freeboard of furnaces for continuous monitoring, regulation and control of the off-gas pressure.

Charge materials are continuously introduced into the furnace. Despite restrictions in amount of fines that are fed to the furnace, percentage of fines is always fed among others because of attrition during transport to the furnace. Since there is an upward flow of process off-gas towards the furnace uptakes on the roof, the fine particles flow together with the gas into the furnace off-gas handling system. Therefore, the furnace off-gas is a mixture of different gas species and fine particles which should be removed using the venturi gas scrubbers. The fine particles can accumulate in different zones in the freeboard and along the off-gas channels.

Another operational phenomenon in submerged arc furnaces is eruption of process gases (sometimes including slag) close to one of electrodes during furnace operation. This phenomenon can be explained as a result of falling of cold and unreacted or partly reacted charge materials into high temperature zone of the furnace. This phenomenon causes release of high temperature process gas around the electrode and hence rapid changes in the off-gas pressure in the freeboard. It has been evidenced by several temperature profiles in the burden near the electrodes [2].

In order to have an optimal operation of the furnace off-gas system it is necessary to have comprehensive understanding of the governing operational conditions. Making a model of the off-gas system with reasonable accuracy can be very helpful. Having access to such tool will make it possible to study effect of different operational phenomena and geometrical aspects on the performance of the system. Therefore the model can be used for improving the current system through modification of the operational methods or geometrical changes. At the same time it can be used as a tool for better design of the system in future.

In the current work a 3D CFD model of the gas and particles flow in the first part of furnace off-gas system starting from the charge surface under the furnace cover and ending before the first stage of venturi gas scrubbers, has been developed. Geometry of the model has been taken from an industrial size furnace in Eramet Norway. The model can simulate operational conditions of the furnace off-gas system. Different parameters such as off-gas temperature, velocity, pressure and distribution of solid fine particles both under the furnace cover and in the off-gas channel can be ob-

tained from its results. Geometrical and operational parameters used in the model can be adapted in order to use the model for other furnaces.

## 2 Description of the CFD model

The furnace off-gas system consists of a chain of different parts such as off-gas uptakes, venturi gas scrubbers, gas filters and MRU. Each part of the system has its own special function and complexities. Making a CFD model of the whole off-gas handling chain is very complicated. The scientific approach which is widely used in CFD modeling of such systems is making separate model of each part rather than modeling of the whole system. The results obtained from each part can then be used as initial or boundary conditions for making a model of the next part. This method has been proved to be an efficient solution for modeling of these types of systems.

The model has been developed to simulate the gas and particles flow both in the freeboard of the furnace and in the off-gas channel before the first stage of the Venturi gas scrubbers. The CFD model is 3D and it includes gas phase which is composed of different species and fine particles which have been considered as a dispersed phase.

### 2.1 Geometry of the model

The model has been built based on dimensions of an industrial FeMn furnace. It starts from the charge surface inside the furnace and it ends up just before the first stage of Venturi gas scrubbers. Geometry of the model which includes furnace body, off-gas uptakes, electrodes and charging chutes is shown in Figure 2.

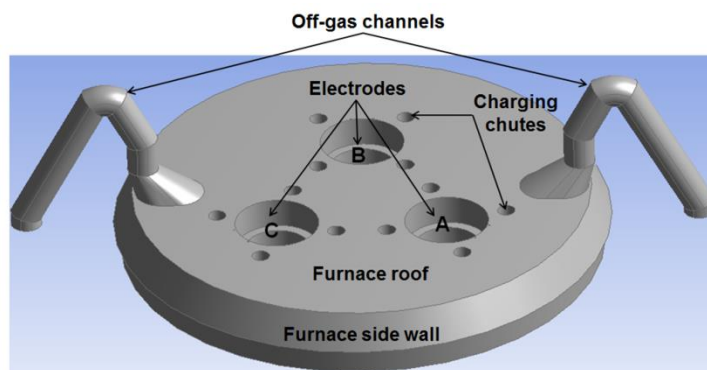


**Figure 2:** Geometry of first part of the furnace off-gas system which is used for modeling

As it is seen from this figure there are gas uptakes in both sides of the furnace close to A and C electrodes and both of them are normally in operation. The furnace has four charging chutes around each electrode through which raw materials are introduced into the furnace.

#### 2.1.2 Charge surface in the furnace

Charge surface inside the furnace is not flat and it is influenced by a position of the charging chutes. In fact, since the charge materials introduced into the furnace are of granular origin, a conical bulk of the newly added raw materials is formed on the charge surface just under the charging chutes. Figure 3 represents the conical shape of charge materials surface inside the furnace.

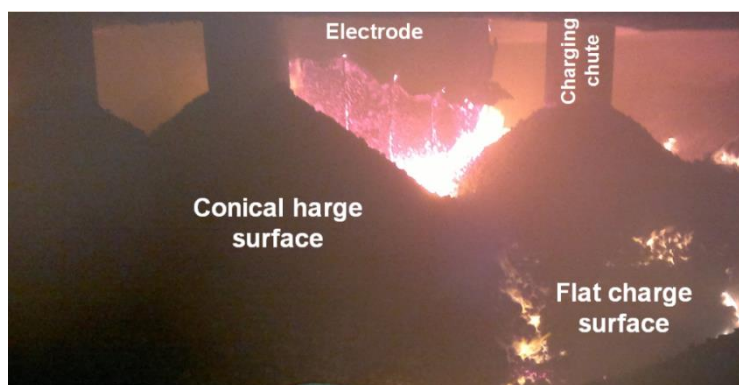


**Figure 3:** Formation of conical charge surface under the charging chutes inside the furnace

The conical surfaces on the charge surface have been considered in the geometry of the model.

## 2.2 Model governing equations

The CFD model is about a mixture of different gas species and fine particles of raw materials in the gas phase. The particles as the second phase in the mode interact with the gas phase, hence, a representative simulation of the off-gas flow in the system is created. The governing equations for mass, momentum and energy conservation for each phase are explained in this section. In addition to these, submodels describing turbulence and radiation have been described as well.

### 2.1.2 Transport equations

The equations which are solved in the CFD model are the continuity, momentum and energy equations. These equations are presented as the following general transport equation [3].

$$\frac{\partial}{\partial t}(\rho\phi) + \nabla \cdot (\rho\phi\mathbf{u} - \alpha\Gamma_{\phi}\nabla\phi) = S_{\phi} \quad (1)$$

Where  $\phi$  represents the variables solved in the model such as mass, velocity and energy,  $\rho$  is the density of fluid,  $\Gamma_{\phi}$  is the effective diffusion coefficient and  $S_{\phi}$  is the source term.

### 2.2.2 Momentum conservation for gas phase

Conservation of momentum in an inertial (non-accelerating) reference frame is described by following equation. The momentum equation (Navier-Stokes equation) satisfies Newton's second law; the rate of change of momentum equals the sum of forces acting on an element.

$$\frac{\partial}{\partial t}(\rho\vec{v}) + \nabla \cdot (\rho\vec{v}\vec{v}) = -\nabla p + \nabla \cdot (\vec{\tau}) + \rho\vec{g} + \vec{F} \quad (2)$$

Where  $p$  is the static pressure,  $T$  is the stress tensor, and  $\rho\vec{g}$  and  $\vec{F}$  are the gravitational body force and external body forces (e.g., that arise from interaction with the dispersed phase), respectively.

### 2.3.2 Energy conservation for gas phase

The energy conservation equation satisfies the first law of thermodynamics; the rate of change of energy equals the sum of the rate of heat addition to and the rate of work done on a fluid element. It is given by:

$$\frac{\partial}{\partial t}(\rho E) + \nabla \cdot (\vec{v}(\rho E + p)) = -\nabla \cdot \left( k_{eff}\nabla T - \sum_j h_j\vec{j}_j + (\vec{\tau}_{eff} \cdot \vec{v}) \right) + S_h \quad (3)$$

The first term in the left hand of Equation (4) is the rate of increase of enthalpy in fluid element; the second term is the convective heat into the fluid element. The first term in the right hand represents the energy transfer due to conduction, species diffusion and viscous dissipation. The second term in the right hand is the volumetric heat source. In which  $E$  is total energy,  $k_{eff}$  is effective conductivity,  $J_j$  is diffusion flux of species  $j$ ,  $S_h$  is heat source and  $h_j$  is species enthalpy.

### 2.4.2 Turbulent model for gas phase

Due to turbulent nature of the process under consideration, the standard k- $\omega$  turbulent model was used in this work. The standard k- $\omega$  turbulence model is an empirical model based on model transport equations for the turbulence kinetic energy (k) and the specific dissipation rate ( $\omega$ ), which can also be thought of as the ratio of  $\omega$  to k [4].

### 2.5.2 Radiation model

The gas radiation in this study is modeled by using the standard P1 model. The P1 radiation model is based on the expansion of the radiation intensity into orthogonal series of spherical harmonics. The radiative flux is given by Eq. (4) where G is the incident radiation and C is the linear-anisotropic phase function coefficient [5, 6].

$$q_r = -\Gamma \nabla G \quad (4)$$

$$\Gamma = \frac{1}{(3(\alpha + \sigma_s) - C\sigma_s)} \quad (5)$$

The transport equation for G is defined in equation (6) where  $\sigma$  is the Stefan-Boltzmann constant and  $S_G$  is a user-defined radiation source.

$$\nabla \cdot (\Gamma \nabla G) - \alpha G + 4\alpha\sigma T^4 = S_G \quad (6)$$

### 2.6.2 Governing equations on the particle phase

In addition to solving transport equations for the continuous phase, we have simulated a discrete second phase in a Lagrangian frame of reference. This second phase consists of spherical fine particles dispersed in the continuous phase. The coupling between the phases and its impact on discrete phase trajectories has been included. Since concentration of the particles in the gas phase is very low, we are allowed to apply Discrete Phase Model (DPM) in the present simulations.

### 2.7.2 Equations of motion for particles

The DPM method predicts the trajectory of a discrete phase particle by integrating the force balance on the particle, which is written in a Lagrangian reference frame. This force balance equates the particle inertia with the forces acting on the particle, and can be written as [7]:

$$\frac{d\vec{U}_p}{dt} = F_D (\vec{U} - \vec{U}_p) + \frac{\vec{g}(\rho_p - \rho)}{\rho_p} + \vec{F} \quad (7)$$

Where  $F_D(\vec{U} - \vec{U}_p)$  is the drag force per unit particle mass,  $u$  is the fluid phase velocity,  $u_p$  is the particle velocity,  $\mu$  is the molecular viscosity of the fluid,  $\rho$  is the gas density,  $\rho_p$  is the density of the particle. Additional forces,  $\vec{F}$ , in the particle force balance can be "virtual mass" force, "Thermophoretic Force", "Brownian Force" and "Saffman's lift force".

### 2.8.2 Heat transfer between gas and particle phases

DPM model uses a heat balance based on following equation in order to relate the particle temperature,  $T_p(t)$ , to the convective heat transfer and the absorption/emission of radiation at the particle surface [7]:

$$m_p c_p \frac{dT_p}{dt} = h A_p (T_\infty - T_p) + \epsilon_p A_p \sigma (\theta_R^4 - T_p^4) \quad (8)$$

Where  $m_p$  is mass of the particle,  $c_p$  is heat capacity of the particle,  $A_p$  is surface area of the particle,  $T_\infty$  is local temperature of the continuous phase,  $h$  is convective heat transfer coefficient,  $\epsilon_p$  is particle emissivity,  $\sigma$  is Stefan-Boltzmann constant and  $\theta_R$  is the radiation temperature.

## 2.3 Properties of the furnace off-gas

Different parameters such as compositions of ores mixture and reductants and the furnace operation can directly affect the off-gas properties. Since the working fluid in the CFD model is the furnace off-gas therefore it is very important to consider precise properties for the furnace off-gas. There is no doubt that the off-gas properties vary with time. However in this work we have tried to make the basic model based on the most common properties of the furnace off-gas.

### 3.1.2 The off-gas composition

Physical properties of the gas phase such as density and viscosity are depended on the gas components and temperature. Typical composition of the gas species in the furnace off-gas is given in Table 1.

**Table 5:** Composition of the furnace off-gas considered in the CFD model

Gas component	CO	CO <sub>2</sub>	H <sub>2</sub>	N <sub>2</sub>	O <sub>2</sub>
Vol. % in the off-gas	62	24	8.5	4	0.5

Average temperature of the off-gas on the charge surface also varies with time, however an average temperature of 523°K (250°C) has been assumed in the CFD model. Viscosity and density of gas mixture at any temperature,  $0 < T < 555^\circ\text{K}$ , has been calculated. Temperature dependent functions have later been used in the CFD model.

### 3.2.2 Particles in the furnace off-gas

The sludge composition has been used as a representative for composition of the fine particles in the furnace off-gas (see Table 2).

**Table 6:** Composition of fine particles in the furnace off-gas

Components	MnO	SiO <sub>2</sub>	Al <sub>2</sub> O <sub>3</sub>	FeO	CaO	MgO
Mass fraction	0.45	0.32	0.11	0.08	0.03	0.01

Size distribution of the particles in the off-gas is given in Table 3. The distribution has been obtained from data available on fines (below 50 μm) content of the raw materials.

**Table 7:** Size distribution of fine particles in the furnace off-gas

Size distribution in the fines (< 50 μm)	20-50 μm	10-20 μm	5-10 μm	< 5μm
	18.6 %	8.9 %	0.2 %	72.3 %

## 2.4 Distribution of the furnace off-gas on the charge surface

The furnace off-gas is not evenly distributed on different zones over the charge surface in the furnace [10, 11]. Direct measurement of spatial flow distribution of the furnace off-gas on the charge surface is not an easy task to be performed. Consumption rate of charge materials in the furnace is not also evenly distributed. In fact, consumption rate of charge materials in the furnace and hence off-gas release is higher close to electrodes compared to the zones near the furnace side wall (see Figure 4(a) [11]).

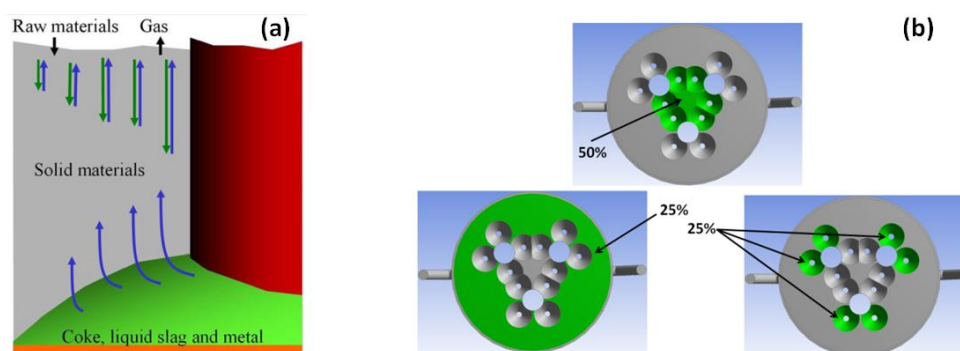


**Figure 4:** (a) Uneven flow of charge materials and reduction gas along an electrode in a furnace [11] and (b) off-gas distribution considered on the charge surface in the CFD model

In the present work we have related the off-gas distribution on the charge surface to the consumption rate of raw materials in different zones of the furnace. As a typical case study in the present work the charge surface has been divided into three different zones. These zones together with off-gas flow distribution on the charge surface are shown in Figure 4(b).

## 2.5 Numerical method and boundary conditions

The numerical approach is used in this study. In order to solve the governing mathematical equations based on finite volume (FVM) method, the commercial CFD software ANSYS Fluent 14.0 has been used. The transport equations for mass, momentum and energy together with described equations of heat transfer, and turbulent flows for both phases (using DPM model) are solved at the same time. The geometry has been divided into 1.5 million of meshes including very fine meshes in outlets of the off-gas channel as well as on the furnace charge surface where the process gas and particles are released.

The average volume of the furnace off-gas from the furnace is 10000 Nm<sup>3</sup>/hr which is distributed on the charge surface. Fine particles distribution on the charge surface has been considered to be even on the whole surface. The off-gas temperature in central zones of the charge surface has been considered 250°C while in the zone which is close to the furnace wall it is 200°C. Water cooling is used for the furnace wall, roof and off-gas channels.

## 3 Results and discussions

The CFD model of the furnace off-gas system simulates pressure, temperature and velocity distribution both in the furnace freeboard and the off-gas channel in different operational conditions. Trajectories of fine particles in the off-gas system show distribution of particles in the off-gas system and hence it is possible to determine zones of the system having high potential for particles to be accumulated.

### 3.1 The off-gas pressure in the freeboard

The off-gas pressure in the freeboard is an important parameter which is continuously monitored. When the off-gas pressure is within a defined range depending on the furnace control strategy, it is normally a sign of stable furnace operation. Frequent variations in the pressure out of the defined range are usually a symptom of unstable operational condition. Figure 5 shows typical measurement of the off-gas pressure in freeboard of the furnace in a period of one day. As it can be seen from this figure there are rapid variations in the off-gas pressure which are mostly related to the eruption charge phenomenon in the furnace. The average off-gas pressure in the freeboard is 0 - 50Pa.

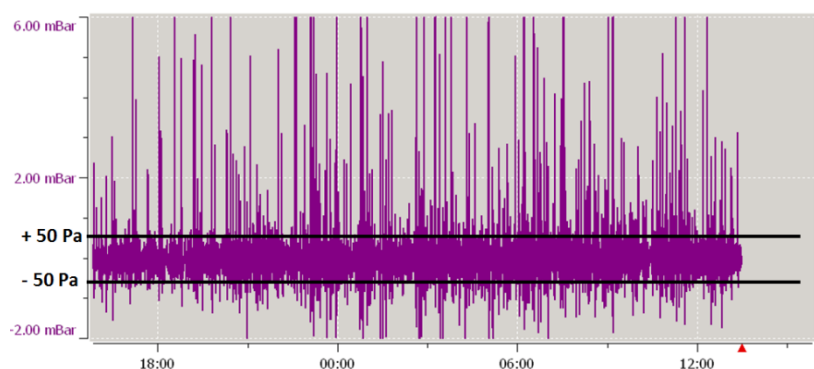


**Figure 5:** Measured off-gas pressure in freeboard of the furnace for 24 hours period of time

Result of the model for pressure distribution in the system is shown in Figure 6. As it is seen from this figure, the pressure distribution in the freeboard is very homogeneous and it is in the range of measured pressure.

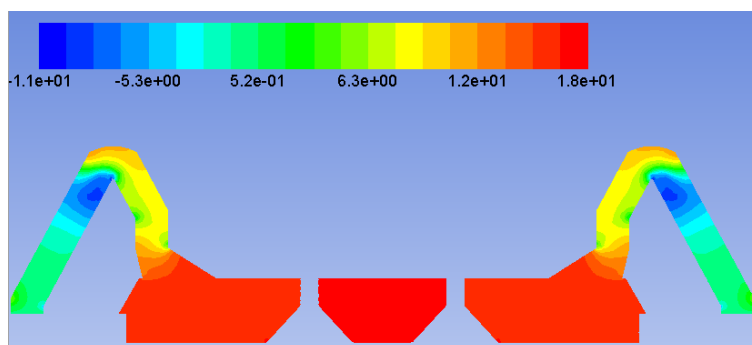


**Figure 6:** Contours of pressure (Pa) distribution in the central vertical plane of the off-gas system.

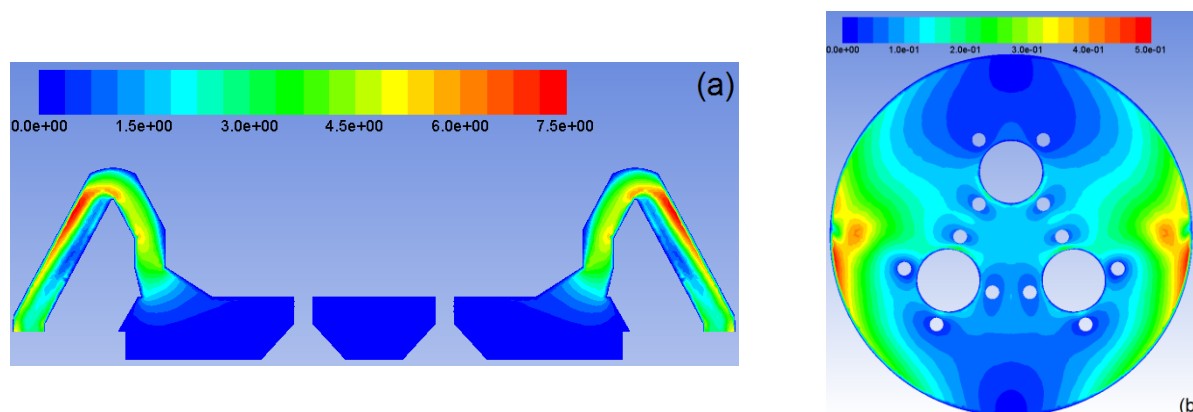
### 3.2 Velocity and temperature distribution in the off-gas system

Figure 7 represents contours of velocity distribution in the off-gas system. Zones of the off-gas channel with low velocity distribution have high potential for particles accumulation and hence clogging phenomenon. The average off-gas velocity at the outlets of the channel is 4.05 m/s.

Result of the model for temperature distribution in the off-gas is shown in Figure 8. As it is seen from this figure the off-gas has higher temperature in the furnace center and of course in the zones in vicinity of the charge surface.

### 3.3 Particles flow in the off-gas system

Fine particles in the off-gas normally follow the gas phase in the system. In this respect particles size is the most important parameter. Figure 9 represents distribution of the fine particles in different zones of the furnace off-gas system



**Figure 7:** Contours of velocity (m/s) distribution in the (a) central vertical and (b) horizontal plane of the furnace off-gas system.

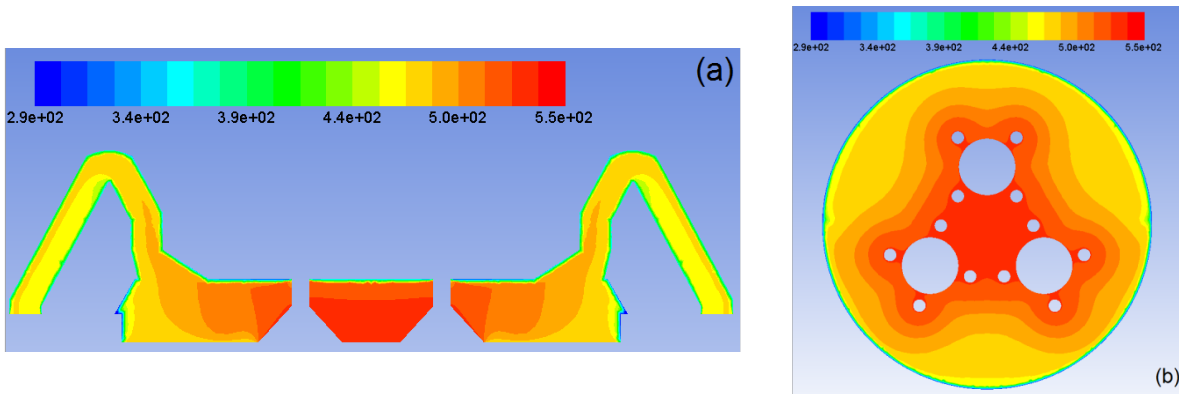


**Figure 8:** Contours of temperature ( $^{\circ}\text{K}$ ) in the (a) central vertical and (b) horizontal plane of the furnace off-gas system.

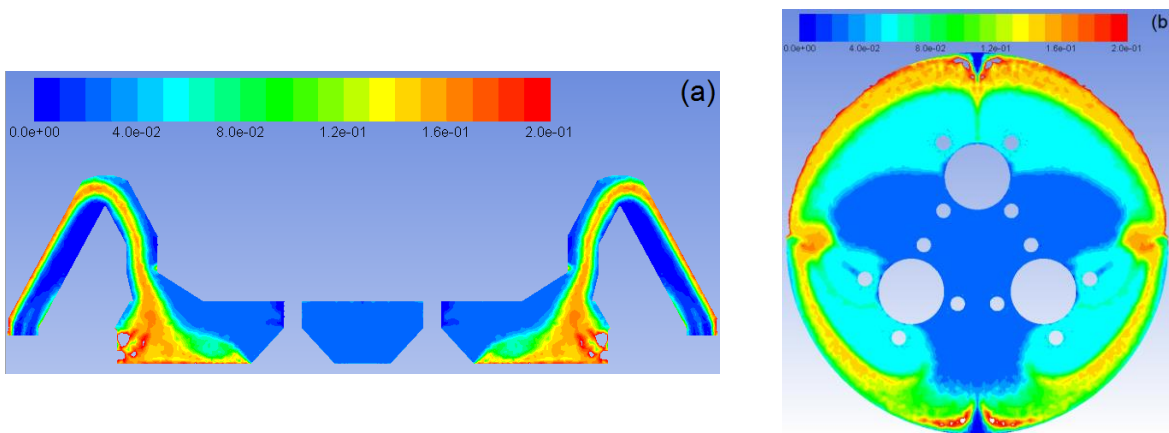


**Figure 9:** Particles concentration ( $\text{kg}/\text{m}^3$ ) in the off-gas system (a) central vertical plane and (b) horizontal planes 1m above charge surface respectively.

This figure shows that particles concentration close to the furnace wall is much higher comparing to the central zone of the furnace. The results show that 59% of the fine particles which are released from the charge surface leave the furnace. The rest is accumulated in the furnace.

Figure 10 represents particles distribution exiting the furnace off-gas system in the case with two gas uptakes. As it is seen from this figure, only small particles (below  $5\mu\text{m}$ ) exit the furnace and bigger particles are accumulated in the furnace either on the charge surface or on the walls.

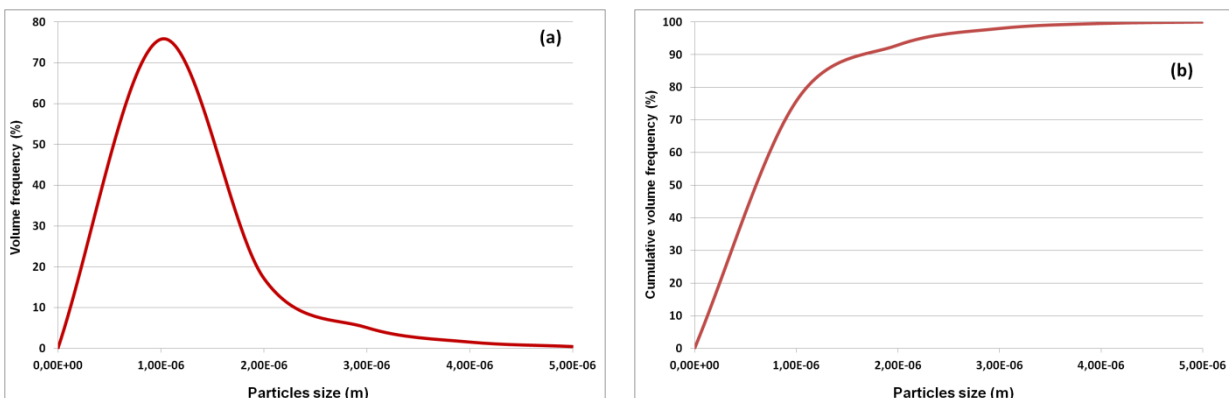


**Figure 10:** Particles distributions (both volume frequency (a) and cumulative volume (b)) which exit the furnace off-gas including two uptakes.

It should be mentioned here that 72.3% of the particles considered in the model have sizes below 5 $\mu\text{m}$  (look at particles distribution in Table 5). It means that in this case in addition to particles bigger than 5 $\mu\text{m}$ , 13.3% of particles with size below 5 $\mu\text{m}$  are also accumulated in the furnace.

Results of previous studies on particles distribution in dried sludge from the furnace show that 96% of the particles obtained in the sludge have a particles distribution below 5  $\mu\text{m}$  which is in a very good agreement with the results obtained from the CFD model.

### 3.4 Pressure variation due to eruption phenomenon in the furnace

As it was described earlier because of eruption phenomenon near electrodes in the furnace very rapid and large variations in the measured off-gas pressure in the freeboard are observed. This phenomenon has been simulated using the developed CFD model.

The results of the CFD model with steady state method show that the off-gas pressure distribution in the freeboard of the furnace is homogeneous. The rapid variation of the off-gas pressure in the freeboard is an implication of transient nature of the eruption phenomenon. Therefore, it is not possible to simulate such phenomenon using previously applied steady state modeling method. The method used for simulating this phenomenon is a combination of steady state and transient methods. In the first stage of modeling the steady state method was used for simulating the system under ordinary operational conditions. In the next step the results of steady state solution were used as initial boundary conditions for transient simulation of the eruption phenomenon.

In order to make a model of this phenomenon we have considered release of high velocity and high temperature off-gas from one side of B electrode in the furnace. Temperature of the released off-gas has been considered 1273 $^{\circ}\text{K}$ . The off-gas velocity in this case has not been measured but we have considered 50 times higher than the normal off-gas velocity which is released from this zone of the charge surface.

Variation of the off-gas pressure with time in different zones of the freeboard has then been monitored. Positions of the zone with high off-gas velocity as well as monitored points have been shown in Figure 11(a). For all these points different heights above the charge surface have been considered.

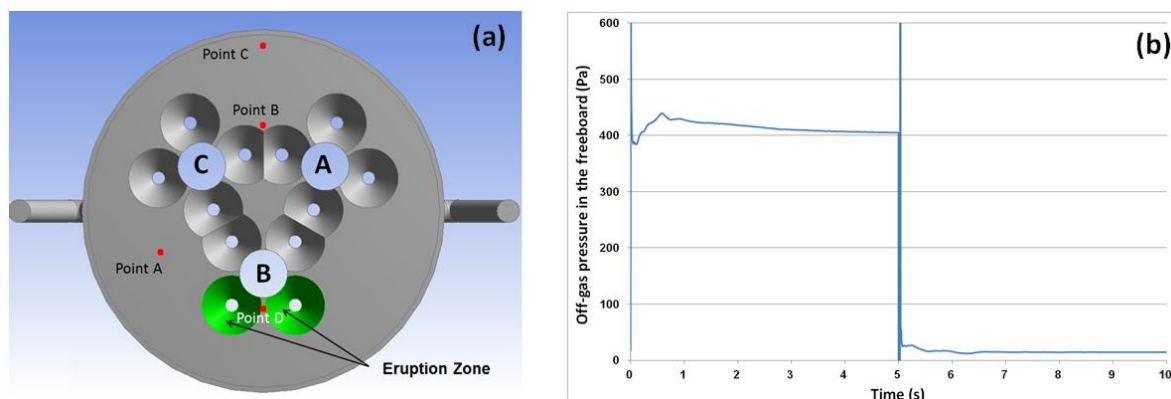


**Figure 11:** Positions of eruption zone near B electrode as well as points in the freeboard where the off-gas pressure has been monitored (a) and Evolution of the off-gas pressure in Point A 1m above the charge surface when the eruption phenomenon occurs in the furnace (b).

Results of the model for pressure simulation during eruption phenomenon at Point A have been presented in Figure 11(b). As it is seen from this figure, the off-gas pressure increases to almost 10 mbar just after eruption phenomenon happens. There is almost no delay in occurring of eruption phenomenon and observation of pressure increase in the measuring point. The pressure then decreases down to 4.3 mbar and remains constant.

As soon as the eruption phenomenon is over (after 5 seconds in current simulation) and the off-gas velocity and temperature return back to their normal level, the off-gas pressure drops (even to a negative value) and increases dramatically. This phenomenon happens because of shocking effect of such sudden decrease in the off-gas velocity. However after a very short time when this shocking effect disappears, the off-gas pressure drops down to the normal value which we had before the eruption happens.

## 4 Conclusions

Gas and fine particles flow in the first part of furnace off-gas system has been investigated through developing a CFD model of the system. Industrial information which are representative enough of the real operation have been in different stages of modeling process. Using the model off-gas pressure, temperature, velocity and particles distribution both in the freeboard of the furnace and in the off-gas channels have been simulated. The results show that a large por-

tion of fine particles which are added to the furnace together with charge materials leaves the furnace through off-gas flow. The model simulates very rapid changes in the off-gas pressure in the freeboard when eruption phenomenon occurs in the furnace. Results also show that the increase in the off-gas pressure in the freeboard is rapidly distributed evenly as well. The model can be used as a tool for investigation of different phenomena which happen in the off-gas handling system. It can also be used as a tool for investigation of the system performance through making different geometrical and operational changes in the system and hence a tool in order to make optimal design of the off-gas system in the future.

## 5 References

- [1] M. Eissa, H. El-Faramawy, A. Ahmed, S. Nabil and H. Halfa, Parameters affecting the production of high carbon ferromanganese in closed submerged arc furnaces, *Journal of Minerals and Materials Characterization & Engineering*, Vol. 11, No. 1, pp. 1-20.
- [2] Report from HATCH, Eramet Norway SAF gas handling debottlenecking study, Eramet Norway internal report 2011-04.
- [3] S. V. Patankar, *Numerical Heat Transfer and Fluid Flow*, Hemisphere Publishing Corporation, New York, 1980.
- [4] D. C. Wilcox, *Turbulence modeling for CFD*, DCW Industries, Inc., La Canada (1998), California, 1998.
- [5] P. Cheng, Two-dimensional radiating gas flow by a moment method. *AIAA Journal*, 2:1662– 1664, 1964.
- [6] R. Siegel and J. R. Howell, *Thermal radiation heat transfer*, Hemisphere Publishing Corporation (1992).
- [7] *Fluent 6.3 user's guide*, 2003, 1077-1080.
- [8] Report from HATCH, Eramet Norway sludge treatment concept study-Phase 1 Final study report, Eramet Norway internal Report 2011-13.
- [9] Report from Eramet Research, 15000 T washing, screening and crushing test of Moanda Ore in Kvinesdal, Start-up assistance, Report 68.09.013-DR.
- [10] V. I. Gusev, V. Ya. Khrolenko, A. L. Sysolyatin, A. Yu. Zilberman and D. V. Kravchenko, Scientific foundation for the production of carbothermal manganese alloys, *Metallurgist*, 2011, Vol. 55, Nos. 3-4, pp. 187-195.
- [11] S. E. Olsen, M. Tangstad, and T. Lindstad, *Production of manganese ferroalloys*, Tapir Academic Press (2007).